Society For Biomaterials

Adhesive and Robust Multilayered Poly(lactic acid) Nanosheets for Hemostatic Dressing in Liver Injury Model

Takuya Komachi,[1] Hideaki Sumiyoshi,[2] Yutaka Inagaki,[2] Shinji Takeoka,[3] Yu Nagase,[1] Yosuke Okamura[1,4]

[1]Course of Industrial Chemistry, Graduate School of Engineering, Tokai University. 4-1-1 Kitakaname, Hiratsuka, Kanagawa 259-1292, Japan
[2]Department of Regenerative Medicine, Tokai University School of Medicine, Kanagawa, Japan
[3]Department of Life Science and Medical Bioscience, School of Advanced Science and Engineering, Waseda University, TWIns, Tokyo, Japan
[4]Micro/Nano Technology Center, Tokai University. 4-1-1 Kitakaname, Hiratsuka, Kanagawa 259-1292, Japan

Received 13 November 2015; revised 20 April 2016; accepted 1 May 2016
Published online 00 Month 2016 in Wiley Online Library (wileyonlinelibrary.com). DOI: 10.1002/jbm.b.33714

Abstract: Freestanding biodegradable nanosheets composed of poly(L-lactic acid) (PLLA) have been developed for various biomedical applications. These nanosheets exhibit unique properties such as high adhesiveness and exquisite flexibility; however, they burst easily due to their nanometer thickness. We herein describe a freestanding, multilayered nanosheet composed of PLLA fabricated using a simple combination procedure: (i) multilayering of PLLA and alginate, (ii) gelation of the alginate layers, (iii) fusion-cut sealing, and (iv) elution of the alginate layers. The multilayered nanosheets not only reinforced the bursting strength but also provided a high level of adhesive strength. In fact, they were found to show potential as a hemostatic dressing, and they tended to show reduced tissue adhesion that accompanies liver injury. Therefore, we propose this biomaterial as a candidate for an alternative to conventional therapy in hemorrhage. © 2016 Wiley Periodicals, Inc. J Biomed Mater Res Part B: Appl Biomater 00B: 000–000, 2016.

Key Words: poly(lactic acid), nanosheet, multilayer, hemostatic dressings, liver injury

How to cite this article: Komachi T, Sumiyoshi H, Inagaki Y, Takeoka S, Nagase Y, Okamura Y. 2016. Adhesive and Robust Multilayered Poly(lactic acid) Nanosheets for Hemostatic Dressing in Liver Injury Model. J Biomed Mater Res Part B 2016:00B:000–000.

INTRODUCTION

Freestanding ultrathin films, often called nanosheets or nanomembranes, have recently attracted much attention as new two-dimensional nanomaterials in the field of nanotechnology.[1,2] These nanosheets represent unique properties such as a high degree of transparency and amazing flexibility due to their large surface area-to-aspect ratio (several centimeter in size but only tens of nanometers in thickness). A large number of techniques to fabricate nanosheets have been proposed that utilize polymers, inorganic materials or their combination, for example layer-by-layer of polyelectrolytes and/or inorganic materials with opposite net charges,[3,4] cross-linking of self-assembled monolayers,[5] Langmuir–Blodgett films with amphiphilic polymers,[6] and a sol–gel process for interpenetrating network nanomembranes.[7] These nanosheets have been applied in a wide variety of fields, for example, electrochemical research and separation technologies, such as sensors, energy storage, and selective adsorption techniques, that take advantage of the ability of nanosheets with large surface areas to provide a high reaction efficiency per unit weight.[1]

For biomedical applications, we have proposed the use of biocompatible nanosheets composed of polysaccharides, such as sodium alginate and chitosan, generated using a layer-by-layer method.[8–10] Moreover, we have also developed biodegradable nanosheets composed of typical polyester series such as poly(L-lactic acid) (PLLA) and their copolymers by using simple fabrication processes consisting of a spin-coating and a new peeling technique.[11–13] Such polyesters have been clinically applied as biodegradable sutures[14] and bone screws,[15] and so forth, and they have also been widely investigated as injectable drug carriers.[16,17] Therefore, utilization of biodegradable polyesters provides an efficient route to clinical application of

Additional Supporting Information may be found in the online version of this article.
Correspondence to: Y. Okamura; e-mail: y.okamura@tokai-u.jp
Contract grant sponsor: This work was supported in part by grants of Research Activity Start-up (24800063) from the Japan Society for the Promotion of Science (JSPS) (Y.O.), Innovative Academic Promotional System in Private Schools Capable of Reproducing First-Rate Researchers in Tokai-University, supported from 2010-Special Coordination Funds for Promoting Science and Technology, the Ministry of Education, Culture, Sports, Science and Technology (MEXT) (Y.O.), and a grant of Strategic Research Foundation Grant-aided Project for Private Universities from MEXT (Y.O.).

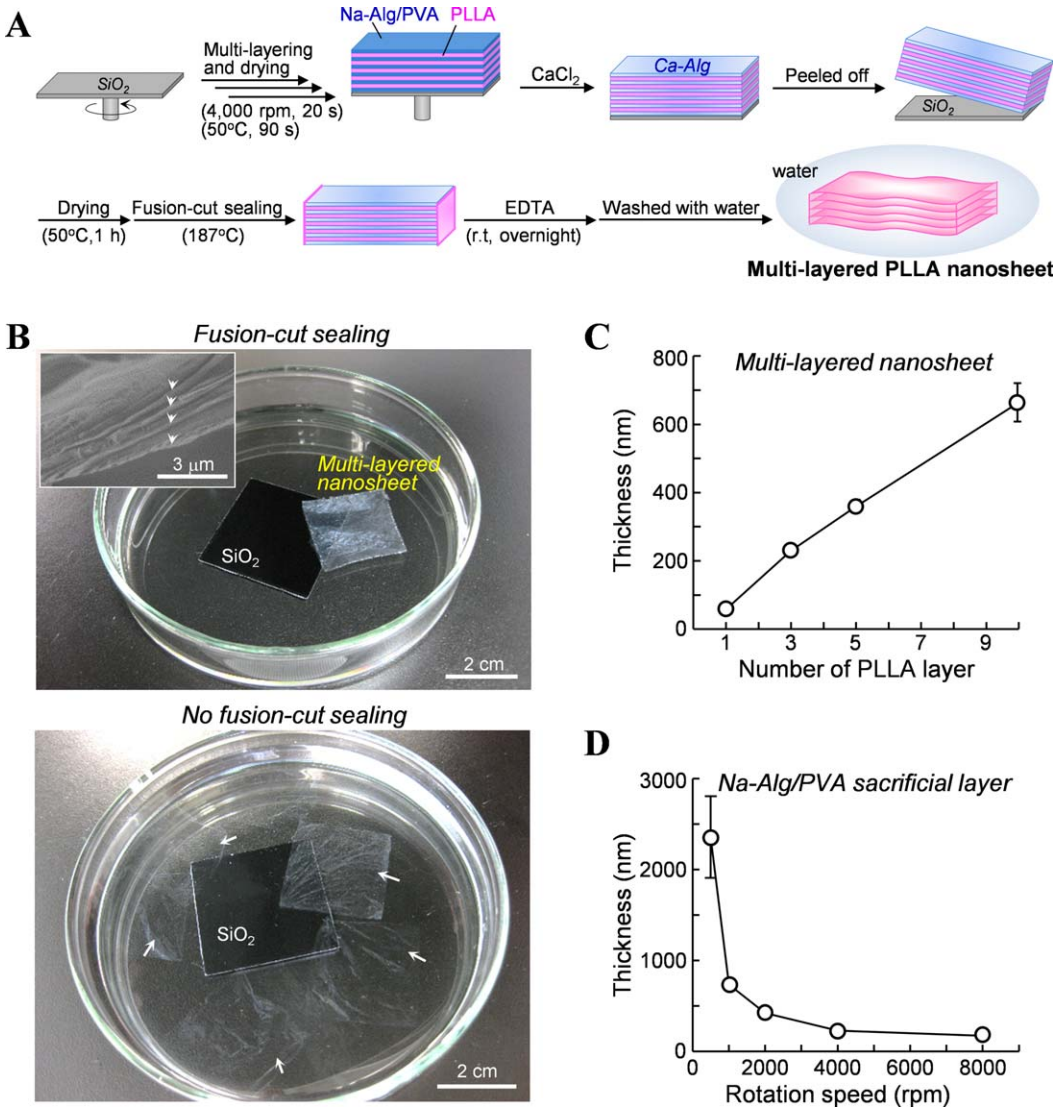

FIGURE 1. Fabrication and characterization of multilayered PLLA nanosheets. (A) Preparative scheme of the multilayered nanosheets by a simple combination procedure: (i) multilayering of PLLA and alginate (Na-Alg/PVA), (ii) gelation of the alginate layers, (iii) fusion-cut sealing, and (iv) elution of the alginate layers. (B) Macroscopic images of the five-layered nanosheet suspended in water after eluting alginate with EDTA (upper panel) and five nanosheets separated discretely in EDTA without the fusion-cut sealing process (lower panel). Inset in the upper panel shows a cross-sectional SEM image of the layer structure. (C) Correlation of the thickness of the multilayered nanosheets with the number of PLLA layers. (D) Correlation of the thickness of Na-Alg/PVA as a sacrificial layer with rotation speed in spin coating.

nanosheets. The PLLA nanosheets exhibited unique properties of flexibility and transparency derived from their nanometer thickness.[11] The greatest benefit of the PLLA nanometer thickness was found to be its high potential to adhere to several different surfaces, such as glasses, steels, plastics, moist skin, and organs, by adding only a little water without any adhesive reagents.[11] Moreover, we demonstrated that the single-layered nanosheets can act as an effective wound dressing, as an alternative to conventional suturing operations in a mouse model.[11] To advance this technology to the next stage, we tested the sealing effects of these nanosheets in large animals. The nanosheets were tightly adhered to various organs; however, they burst easily during bleeding and peristaltic action of the organs, due to their nanometer thickness. This would be a major issue faced by nanosheets designed for biomedical applications. Thickening of the nanosheets should improve their performance. However, this thickening could reduce or remove their advantage of high adhesiveness.[11] This is a central dilemma in the design of the nanosheets.

In this study, we propose a fabrication procedure in which a multilayered PLLA nanosheet is generated. This nanosheet can be handled as a single nanofilm, but it has interior spaces between the multiple layers of the nanosheet. We expected that the high adhesiveness of the nanosheet would be maintained by constraining the thickness of its constituent layers to a nanometer thickness <100 nm. We also expected that its resistance to bursting would be reinforced by the multilayering process. Moreover, we demonstrated that the multilayered nanosheets acted as an

effective hemostatic dressing in a model of liver injury. We herein focused on the liver as a model organ, because of its large size and fragility, and because it bleeds copiously after liver injury. This model established previously[18,19] is an appropriate *in vivo* system to evaluate the resistance to bursting from bleeding and the adhesiveness of multilayered nanosheets applied to organs postsurgery.

MATERIALS AND METHODS

Fabrication of multilayered PLLA nanosheets

Silicon wafers covered with silicon oxide grown thermally (SiO_2 substrate; KST World Co., Fukui, Japan; typical size: 40 mm × 40 mm) were treated with a piranha solution (sulfuric acid:hydrogen peroxide = 4:1, v/v) and then rinsed with distilled water and dried (50°C, overnight). Sodium alginate (Na-Alg, Mw: 106 kDa; Kanto Chemical Co., Tokyo, Japan) and poly(vinyl alcohol) (PVA, Mw: 22 kDa, 89% hydrolyzed; Kanto Chemical Co. or EMPROVE® exp for the *in vivo* study, 85–89% hydrolyzed; Merck KGaA, Darmstadt, Germany) were dissolved in distilled water at a concentration of 20 and 25 mg/mL, respectively. In order to produce a water-soluble sacrificial layer, an aqueous solution of Na-Alg was mixed with 10% volume of an aqueous solution of PVA ([Na-Alg] = final concentration [fc.] 18 mg/mL, [PVA] = fc. 2.5 mg/mL). A solution of Na-Alg containing PVA (1 mL) was pipetted onto the SiO_2 substrates, and the substrates were spin-coated at 4000 rpm for 20 seconds (MS-A150; Mikasa Co., Tokyo, Japan), followed by drying at 50°C for 90 seconds [Figure 1(A)]. Next, PLLA (Mw: 80–100 kDa; Polysciences, Warrington, PA) was dissolved with methylene chloride at a concentration of 10 mg/mL, and the solution (0.7 mL) was pipetted onto the Na-Alg/PVA-coated SiO_2 substrates. The substrates were then spin-coated and dried under the same conditions. For preparation of multilayered PLLA nanosheets, the multilayering process of Na-Alg/PVA and PLLA was repeated 3–10 times by multiple rounds of spin-coating (4000 rpm, 20 seconds) and drying (50°C, 90 seconds). The final layer was coated with Na-Alg/PVA. The obtained substrates were immersed in an aqueous solution of 20 mg/mL $CaCl_2$ (Kanto Chemical Co.) at room temperature (RT) for 30 minutes to allow gelation of the Na-Alg layers between PLLA nanosheets, which temporally assembled into one thick composite film. The film was spontaneously released from the substrates into distilled water and scooped up with nonwoven fabrics composed of polyethylene and polypropylene (Daiso Industries Co., Hiroshima, Japan) and dried (50°C, 1 hour). The dried films were then gently detached from the nonwoven fabrics with tweezers and only two sides of the films were fusion-cut sealed with a Poly sealer® equipped a 2-mm fusion-cut heating element (Model PC-200; Fuji Impulse Co., Osaka, Japan) for ~1 second at different temperatures (preset numbers 4, 5, and 6 were 156, 187, and 213°C, respectively). The sealed films were incubated in 0.5 *M* ethylenediaminetetraacetic acid (EDTA; Kanto Chemical Co.) at RT overnight to dissolve and remove alginate and PVA layers between the PLLA nanosheets. After washing with distilled water overnight, we obtained the multilayered PLLA nanosheets. All fabrication processes were performed in a clean room (class 10,000 conditions) to avoid contamination.

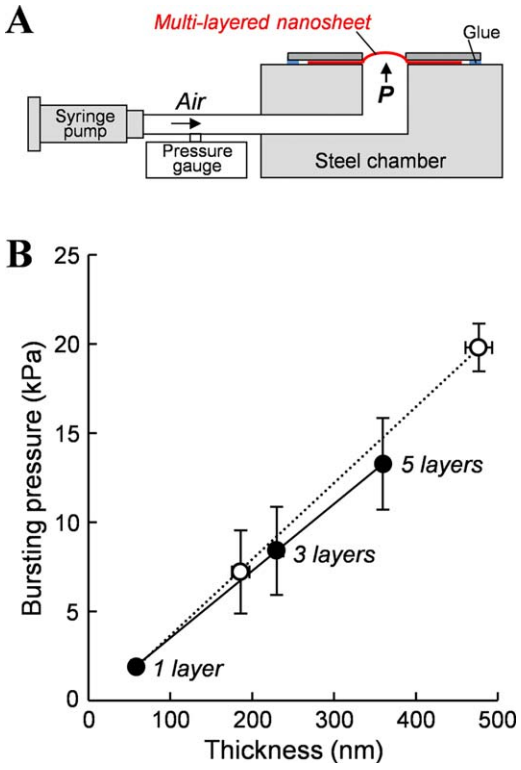

FIGURE 2. Bursting strength of the multilayered PLLA nanosheets. (A) Schematic image of a bursting test to measure the bursting pressure. (B) Correlation of the bursting pressure of the multilayered nanosheets (●) or single-layered nanosheets (○) with their respective thicknesses.

The macroscopic morphologies [Figure 1(B)] of the multilayered nanosheets with or without the fusion-cut sealing process were photographed with a digital camera (IXY DIGITAL 25 IS; Canon, Tokyo, Japan). Cross-sectional image of the nanosheet was recorded with a field emission scanning electron microscope (FE-SEM S-4800; Hitachi High-Technologies Co., Tokyo, Japan) at an accelerating voltage of 1 kV [Figure, 1(B), inset]. To this end, the multilayered nanosheet frozen in liquid nitrogen was broken with tweezers. The broken pieces were fixed with a carbon tape on the stage, to which gold was sputtered at an ionic current of 3 mA for 30 seconds by using a SC-701 Quick coater (Sanyu Electron Co., Tokyo, Japan) prior to observation. The average thicknesses of the multilayered nanosheets and sacrificial layers adhered on the SiO_2 substrate were measured with a Surfcorder T-200 [Kosaka Laboratory, Tokyo, Japan; Figure 1(C,D)]. Each experiment was performed at least three times. Values were given as the mean ± standard deviation (SD). Melting temperatures (T_m) of bulk PLLA and PVA used in this study were measured by a differential scanning calorimetry (DSC, DSC-6200; Seiko Instruments, Chiba, Japan) at a heating rate of 10°C/min under a nitrogen atmosphere.

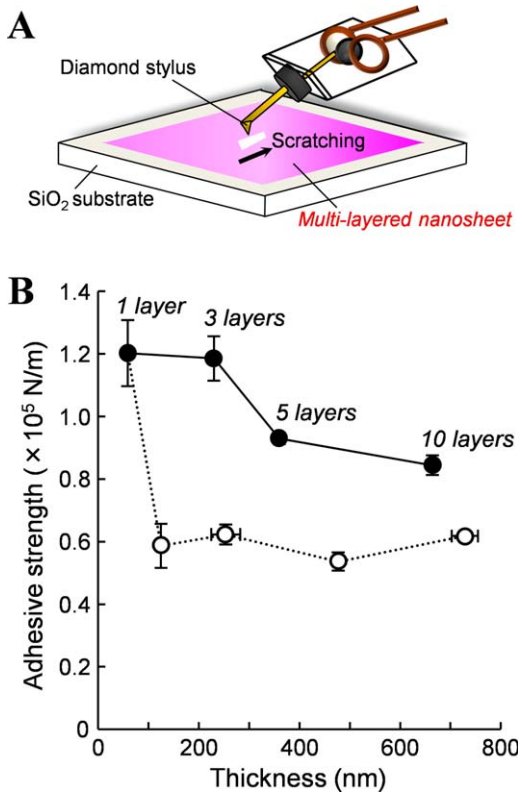

FIGURE 3. Adhesive strength of the multilayered PLLA nanosheets. (A) Schematic image of a microscratch tester for thin films. (B) Correlation of the adhesive strength of the multilayered nanosheets (●) or single-layered nanosheets (○) with different thicknesses adhered on the SiO_2 substrate.

Bursting pressure

The bursting pressure of the multilayered nanosheets with three to five layers was evaluated using a bursting test (Figure 2), which is a modified device established previously.[10,11,20] The nanosheets floating in water were scooped up using a stainless plate with a 2.5-mm circular hole in the center and then dried (RT, overnight) in a desiccator. The plate was fixed on a stainless chamber with glue (aron alpha®, Toagosei Co., Tokyo, Japan). Air was injected into the chamber with a syringe pump (SPS-1; ASONE Co., Osaka, Japan) at a rate of 3 mL/min, and the pressure until bursting of the nanosheets was continuously monitored with a digital manometer (GPG104C; Okano Works, Osaka, Japan). As a control, the bursting pressures of single-layered nanosheets with thicknesses ranging from 59 to 477 nm were measured. The obtained values were averaged for each condition (n = 6–10), and plotted against the thicknesses. Values were given as mean ± SD.

Adhesive strength

The adhesive strengths of the multilayered nanosheets were evaluated with a microscratch tester for thin films (model CSR-2000; Rhesca Co., Tokyo, Japan; Figure 3) as reported previously.[11,21] The multilayered nanosheets consisting of 3–10 layers were adhered on the SiO_2 substrate, followed by drying at RT overnight in a desiccator. The surface of the adhered nanosheets was scratched with a diamond stylus at a curvature radius of 25 μm under optimal conditions (vertical loading rate: 0.17 mN/s, scratch width: 100 μm, scratch rate: 10 μm/s). The critical load was determined from the signal change of frictional vibration just after detaching the nanosheets. The obtained values were corrected for the thicknesses to define the adhesive strength, averaged for each condition (n = 3–5) and plotted against the thickness. We also measured the adhesive strengths of the single-layered nanosheets with thicknesses ranging from 59 to 729 nm. Values were given as mean ± standard error of the mean (SEM).

Liver injury model

All animal experiments were performed according to the guidelines approved by the Animal Experiment Committee of Tokai University. Male Sprague-Dawley rats (6-weeks old, weight 179 ± 18 g; Clea Japan, Tokyo, Japan) were deeply anesthetized with isoflurane (Pfizer Japan, Tokyo, Japan). After laparotomy, the model of liver injury was prepared according to a procedure reported previously.[18,19] Briefly, a plastic template with a 10-mm hole in the center (size: 40 mm × 40 mm, thickness: 3 mm) was impressed on the surface of the left lateral lobe of the liver and the raised liver was resected with a surgical knife (No. 11; ASONE Co., Osaka, Japan). Blood spilled on the liver just after resection was blotted with a medical gauze prior to sealing of the five-layered nanosheet, which was supported with a PVA film having a thickness of about 10 μm [Figure 4(A)]. The nanosheets (size: *ca*. 20 mm × 25 mm) were adhered on petri dishes (90 mm ϕ), to which an aqueous solution of PVA (25 mg/mL, 10 mL) was gently applied, and the petri dishes were dried (50°C, overnight). The dried PVA films transferring the nanosheets were then detached from the petri dishes and cut at a typical size of 25 mm × 30 mm, that is, slightly larger than the nanosheets (margin of PVA on each side: 2.5 mm). The sealing effect of the single-layered nanosheet (thickness: 60 nm) supported with a PVA film was also tested using the same protocol. Blood loss during and immediate after the sealing process was absorbed with cotton swabs for 5 minutes. As negative and positive controls, only the PVA film and TachoSil® (CSL Behring K.K., Tokyo, Japan) were sealed onto the incised liver. Blood loss before and after sealing was calculated by subtracting the weight of the gauzes and cotton swabs, and averaged for each condition [n = 7–8; Figure 4(B)]. Moreover, the weight of the resected liver was measured and plotted for each condition. After sealing, abdominal closure was performed using a biodegradable 4–0 suture (J304H, Vicryl®; Johnson & Johnson K.K., Tokyo, Japan). We next evaluated whether surrounding tissues were adhered to the liver 7 days after surgical intervention [Figure 5(A,B)]. The severity of adhesions was scored according to the following system reported previously[22]: Score 0: no adhesions, Score 1: firm adhesion with easily dissectable plane, Score 2: adhesion with dissectable plane causing mild tissue trauma, Score 3: fibrous adhesion with difficult tissue adhesion, and Score 4: fibrous adhesion with nondissectable tissue planes.

Moreover, the average number of adjacent tissues adhered to the liver was manually counted for each group (n = 7–8). A different researcher performed the scoring of adhesions from the researchers who fabricated the multilayered nanosheets to limit bias. For histological examination to access the fibrogenic response, the livers were excided after evaluating the degree of adhesions, fixed in 10% formaldehyde, and then stained with hematoxylin–eosin (H–E) [Figure 5(C)]. All values were given as mean ± SEM.

Permeation test

Transwell membranes® with a pore size of 8 μm (TMs; membrane diameter: 6.5 mm, Corning Co., NY) were immersed into 5% (w/v) bovine serum albumin (BSA; Mw: 66.5 kDa; Sigma-Aldrich Co., Tokyo, Japan) in phosphate-buffered saline (PBS; pH 7.4) as a blocking agent in a 24-well plate (4°C, overnight). After rinsing with PBS, the single- or five-layered nanosheets were adhered onto the outside of TMs and dried (RT, overnight) (Figure 6). The TMs covered with the nanosheet were set into a 24-well plate filled with 1 mL of PBS. As model analytes, 10 mg/mL solution of rhodamine B (Rho B; Mw: 479 Da, E_x: 570 nm, E_m: 590 nm; Sigma-Aldrich Co.) or BSA labeled with fluorescein isothiocyanate (FITC-BSA,[23,24] E_x: 494 nm, E_m: 518 nm, referred to Supporting material) were utilized for the permeation test. An aliquot of each analyte (200 μL) was pipetted into the inner compartment of the nanosheet-coated TM, which was then incubated at 37°C in a shaking bath (SB-13; ASONE Co.). The amount of analyte that permeated into the outer compartment of the well was continually monitored using a microplate reader for 6 hours (SH-9000Lab; Corona Electronic Co., Ibaraki, Japan) set in the fluorescent mode to detect each dye. The fluorescent intensity was defined as 100% if all of the inner analyte permeated to the outer compartment. The corrected intensities were averaged for each condition (n = 3) and plotted against the incubation time. Values were given as the mean ± SEM. Moreover, the permeation flux was calculated from the corrected permeation curve, with the y-axis converted to show permeation weight instead of percentage using the following equation:

$$\text{Permeation flux}\,(\text{g/m}^2\,\text{h}) = V\,(\text{g/h})/A\,(\text{m}^2)$$

where V is the permeation rate calculated from the slope of the permeation curve, and A is the total area of the pores in the TMs (1.67×10^{-6} m^2).

Statistical analysis

Statistical significance of blood loss and weight changes of the resected livers in each group [Figure 4(B)] was evaluated using the analysis of variance (ANOVA) test, followed by the Tukey–Kramer test. Statistical significance of the score and number of tissue adhesions was evaluated using the Kruskal–Wallis test and then the Steel–Dwass test [Figure 5(B)]. p-Values <0.05 were considered as statistically significant. Statistical analyses were performed with MATLAB (MathWorks, MA) or Microsoft Excel.

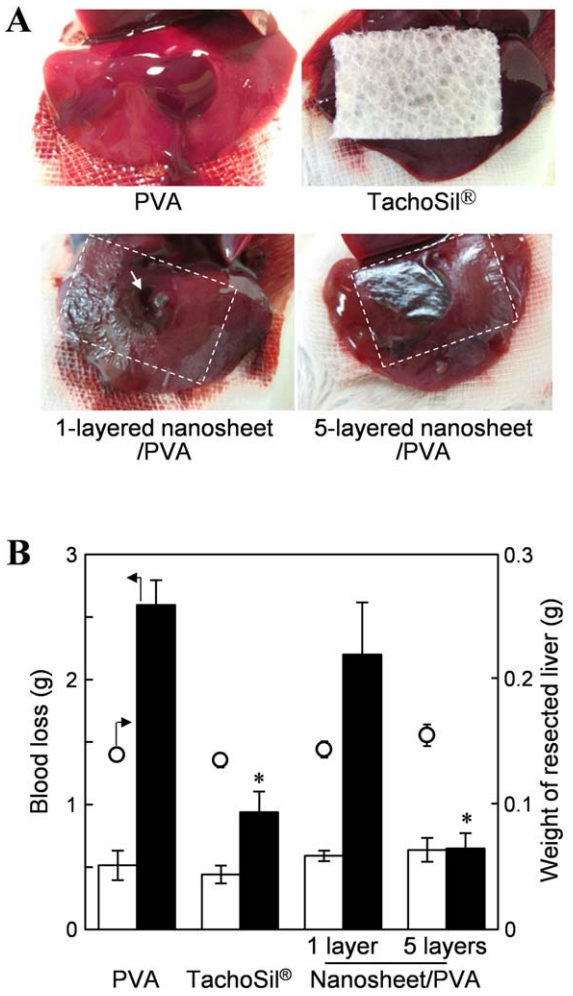

FIGURE 4. *In vivo* sealing effect of the multilayered PLLA nanosheets used in a liver injury model. (A) Macroscopic images of resected livers sealed with only a PVA film, TachoSil®, or one- or five-layered nanosheets supported with PVA film. Broken lines show each nanosheet, and arrow shows the site of rupture. (B) Blood loss before (opened columns) and after (closed columns) sealing with the above materials (n = 7–8). Plots show weight of resected liver in each group. *$p < 0.05$ for TachoSil® or five-layered nanosheet group versus PVA group.

RESULTS

Fabrication of multilayered PLLA nanosheets

The detailed fabrication procedure to create multilayered PLLA nanosheets is depicted in Figure 1A. The first step is a multilayering process of PLLA. We focused on Na-Alg to create an appropriate sacrificial layer between PLLA. However, only Na-Alg was repelled from the hydrophobic surface of the PLLA-coated SiO_2 substrate, although Na-Alg could be spin-coated onto the bare SiO_2 substrate. To improve its performance, a small amount of PVA (fc. 2.5 mg/mL) was mixed with a solution of 20 mg/mL Na-Alg. This mixture was first spin-coated onto the substrate (4000 rpm, 20 seconds), corresponding to a thickness of 231 ± 10 nm in the dry state. A 10 mg/mL solution of PLLA was next spin-coated onto the Na-Alg/PVA-coated substrate under the same conditions, corresponding to a thickness of 59 ± 4 nm. Subsequently, the multilayering process of Na-Alg/

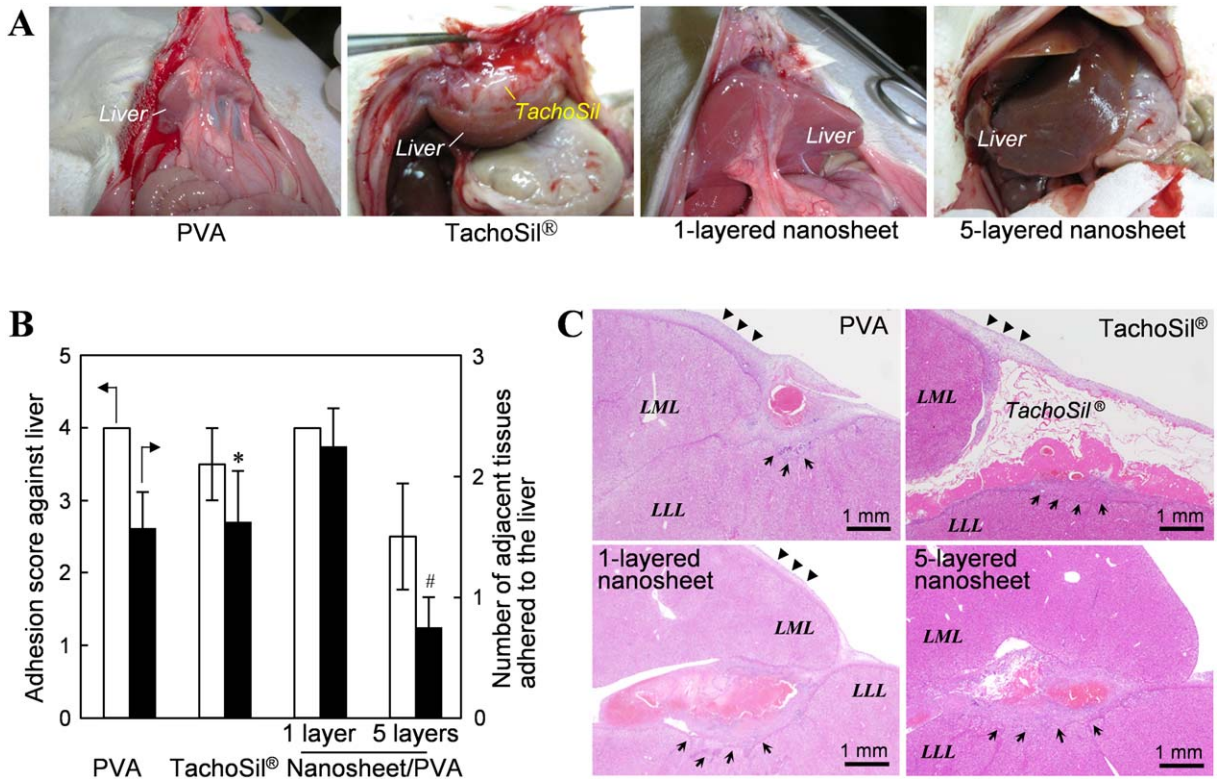

FIGURE 5. Observation of the liver 7 days after surgical intervention. (A) Macroscopic images of the liver sealed with a PVA film, TachoSil®, or one- or five-layered nanosheets. (B) Adhesion score (opened columns) and number of adjacent tissues adhered to the liver (closed columns) in each group (n = 7-8). $^{*}p < 0.05$ for TachoSil® group versus one-layered nanosheet group and $^{\#}p < 0.05$ for the five-layered nanosheet group versus the one-layered nanosheet group. (C) Histological images of the liver stained with H–E in each group. Arrowheads indicate the thick fibrous membranes on the surface of the liver, while arrows represent the original sites of wounding. Letters LLL and LML in the images show left lateral lobe and left median lobe of the liver, respectively.

PVA and PLLA was repeated four times (corresponding to a total of five layers of PLLA nanosheets) on the SiO_2 substrate, and the final layer was coated with Na-Alg/PVA. This small amount of PVA was thus an essential component for multilayering of Na-Alg on PLLA. The second step is a gelation process of the alginate layers. When the obtained

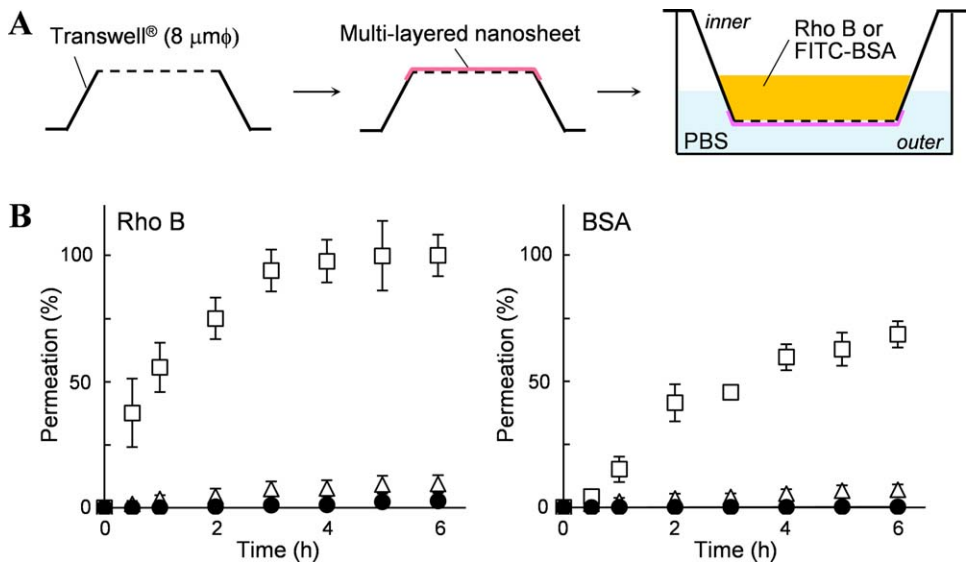

FIGURE 6. Permeation test of the multilayered PLLA nanosheets. (A) Schematic image of the permeability assay using a Transwell Membrane® (TMs) adhered to the nanosheets. (B) Correlation of permeability of the analytes (Rho B and BSA) through the five-layered nanosheets (●) or one-layered nanosheets (△) or bared TMs (□) with time.

substrate was immersed into an aqueous solution with Ca^{2+}, the film surface on the substrate became whitish, indicating that the Na-Alg layers between the nanosheets had turned into insoluble hydrogels. In fact, one thick composite film was released from the substrate into water due to two-dimensional interaction between all of the layers. The third step is a fusion-cut sealing process. The composite film suspended in water was scooped up and dried on a nonwoven fabric cloth. The film was easily detached with tweezers and handled in air due to the thick and robust film. In order to avoid separation of each nanosheet, we utilized a Poly sealer®, by which only two sides of the film were melted and cut, resulting in a fusion of all the composite layers. The T_m of bulk PLLA and PVA obtained from the DSC curve were measured to be 166 and 164°C, respectively. The T_m of bulk alginate was reported to be 182°C.[25] At a preset temperature of 187°C, which is a bit over the T_m of all components in the films, the edges of the film were efficiently fusion-cut sealed. Treatment at 156°C was insufficient for cutting, whereas, treatment at 213°C started to char the sealed parts of the film. We thus demonstrated that the T_m of the composite film components was an important parameter for fusion-cut sealing, and a T_m of 187°C was found to be optimal in this study. The final step is an elution process of the alginate layers. When the fusion-cut sealed film was immersed into an EDTA solution, its configuration was maintained even after washing with distilled water [Figure 1(B)]. On the other hand, the film without fusion-cut sealing was separated into five discrete nanosheets in an EDTA solution due to instant dissolving of the alginate layers between the nanosheets [Figure 1(B)]. Hence, the fusion-cut sealing process was necessary to preserve the configuration of the film, which consisted of five layers.

The obtained film was an amazingly flexible structure, which appeared whitish at various observation angles due to the reflection of light [Figure 1(B)]. This indicates that EDTA had diffused from the nonsealed edges of the film, where it dissolved and eluted the alginate gel layers, resulting in nanosheets with internal multilayers. In fact, cross-sectional SEM observation revealed that the film possesses a layered internal structure [Figure 1(B)]. Fourier Transform Infrared (FT-IR) analysis of the film revealed that almost of the PVA and alginate used as a water-soluble sacrificial layer were removed from the films, based on a band at 3350/cm corresponding to the O–H stretching vibration mode (Figure S1). Furthermore, the number of layers in a nanosheet can be controlled by adjusting the multilayering process of PVA/Na-Alg and PLLA. As described above, the thickness of the single-layered nanosheet was 59 ± 4 nm. If multilayered nanosheets consisting of 3–10 layers were desired, their thicknesses may be estimated simply by multiplying the number of layers by the thickness of the single-layered nanosheet [e.g., 3 layers: 230 ± 8 nm, 5 layers: 360 ± 4 nm, and 10 layers: 664 ± 50 nm; Figure 1(C)]. This result also supports our conclusion that the almost of alginate layers was eluted from the multilayered nanosheets. Furthermore, by spin-coating at different rotation speeds [Figure 1(D)], the thickness of the sacrificial layers could be also constrained from 174 ± 15 to 2357 ± 449 nm, corresponding to the interval regions between PLLA layers. Consequently, we succeeded in fabricating freestanding multilayered PLLA nanosheets using simple procedures: (i) multilayering of PVA/Na-Alg and PLLA, (ii) gelation of the alginate layer, (iii) fusion-cut sealing, and (iv) elution of the alginate layers.

Bursting pressure and adhesive strength

Bursting pressures of the multilayered nanosheets were measured with a bursting tester [Figure 2(A)]. As a reference, the single-layered nanosheets with different thicknesses were utilized. The pressure until bursting of the single-layered nanosheet with a thickness of 59 ± 4 nm was measured to be 2.0 ± 0.1 kPa [Figure 2(B), ○]. The bursting pressures increased proportionally with the thickness of the single-layered nanosheets as expected (7.2 ± 2.3 and 19.8 ± 1.3 kPa at a thickness of 186 ± 11 and 477 ± 16 nm, respectively). When the multilayered nanosheets were then tested using the same procedure, the three- and five-layered nanosheets were more difficult to burst than the single-layered nanosheet with a thickness of 59 ± 4 nm [three layers with total thickness of 230 ± 8 nm: 8.4 ± 2.5 kPa and five layers with total thickness of 360 ± 4 nm: 13.3 ± 2.6 kPa; Figure 2(B), ●]. The obtained fitted curve for multilayered nanosheets against total thickness was correlated with that of the single-layered nanosheets. Hence, we demonstrated that the bursting strength of the multilayered nanosheets could be controlled by adjusting the number of layers.

We next tested the adhesiveness of the multilayered nanosheets using a scratch tester for thin films [Figure 3(A)]. Based on the critical load just after detaching the single-layered nanosheet (thickness: 59 ± 4 nm) from a SiO_2 substrate, the adhesive strength was calculated to be (1.20 ± 0.11) × 10^5 N/m [Figure 3(B), ○]. However, for thicknesses over 100 nm, the adhesive strengths were significantly decreased as reported previously[11] (thicknesses of 125 ± 5, 254 ± 7, 477 ± 16, and 729 ± 45 nm: (0.59 ± 0.07) × 10^5, (0.62 ± 0.03) × 10^5, (0.54 ± 0.03) × 10^5, and (0.62 ± 0.02) × 10^5 N/m, respectively). Next, we evaluated the adhesiveness of the multilayered nanosheets. Intriguingly, individual layers were not detached in a stepwise fashion, rather all of layers detached from the SiO_2 substrate at the critical load simultaneously. The adhesive strength of the three-layered nanosheet was comparable to that of a single-layered nanosheet with a thickness of 59 ± 4 nm, representing a high level of adhesive strength [three layers: (1.19 ± 0.07) × 10^5 N/m; Figure 3(B), ●]. For 5- and 10-layered nanosheets, the adhesive strengths represented still higher levels compared to the single-layered nanosheets with an equivalent thickness [5 layers: (0.93 ± 0.02) × 10^5 N/m and 10 layers: (0.84 ± 0.03) × 10^5 N/m). Consequently, we demonstrated that having multinanolayers in the film was an effective configuration, not only to reinforce the bursting strength but also to provide a high level of adhesive strength.

Sealing effect of multilayered PLLA nanosheets in a liver injury model

We tested whether the multilayered nanosheets could act as a hemostatic dressing in a liver injury model. Prior to *in vivo* testing we estimated how many layers in the nanosheets are necessary to stop bleeding in the following liver injury rat model. Total blood volume of the rat was estimated as 5.6% of total body weight, as reported previously.[26,27] Hence, the total blood volume of rats used in this study was estimated to be ca. 10 mL based on the average body weight of rats (179 ± 18 g). If the multilayered nanosheets could resist pressure applied by a 10 mL of blood oozing from the liver, they could potentially serve as a hemostatic dressing following liver injury. When air or distilled water as a model liquid was injected into the tube, the relationship between injection volume and pressure was basically comparable (Figure S2). Thus the results obtained from experiments with tubes are correlated with those obtained from the bursting test. In the bursting tests, the five-layered nanosheets were found to be resistant until the pressure reached 13.3 ± 2.6 kPa [Figure 2(B)]. By substituting this value into the fitted curve [Figure S2(A)], the injection volume of water just before bursting was estimated to be about 10.1 mL. This indicates that the nanosheet would be unlikely to break even if the total blood volume bleeds (which is clearly unrealistic). In the case of three-layered nanosheets, the injection volume just before bursting was estimated to be about 6.4 mL, suggesting that these nanosheets could possibly burst under physiological bleeding. Next, we also estimated the relationship between the resistance of the nanosheets and the blood pressure in the liver. The blood pressure of hepatic artery in normal rats has been reported to be <70 mmHg (*ca*. 9.3 kPa)[28]. Since the diameter of proximal hepatic artery was about 0.21 mm (area: 3.5×10^{-8} m^2),[28] the force subjected to the nanosheets was calculated to be about 0.33 m*N* if the cutting plane of the artery was directly contacted to the nanosheet. On the other hand, the single-layered nanosheet was found to be resistant until the pressure of about 2 kPa in the bursting test [Figure 2(B)]. This corresponds to a need to break at a force of about 9.8 m*N* from the diameter of the hole used in the test (2.5 mmϕ, area: 4.9×10^{-6} m^2). This indicates that even the single-layered nanosheet is unlikely to burst by the pressure of hepatic artery itself, but the volume of blood oozing from the liver, which was apparently affected by the blood pressure, seemed to be the direct factor to determine the bursting of nanosheet. Based on both estimates, we decided that the nanosheets with at least five layers could potentially act as a hemostatic dressing for liver injury.

The therapeutic sealing effect of the five-layered nanosheet was evaluated using a rat model of liver injury that was established previously.[18,19] To easily handle the five-layered PLLA nanosheet, PVA supporting films to transfer the nanosheet were utilized [Figure 4(A)]. As negative and positive controls, PVA supporting films alone and TachoSil® applied clinically were sealed to the incised liver. Moreover, a single-layered nanosheet supported with PVA films was also tested. When liver injury was performed, the weights of the resected livers were comparable in all groups [Figure 4(B), ○; PVA: 139 ± 4 mg, TachoSil®: 135 ± 5 mg, single-layered nanosheet/PVA: 144 ± 6 mg, and five-layered nanosheet/PVA: 155 ± 9 mg, $p > 0.3$ by ANOVA]. Blood loss estimated from wiping with a medical gauze just before sealing with the above materials was also comparable in all groups [Figure 4(B) open columns; PVA: 0.51 ± 0.12 g, TachoSil®: 0.44 ± 0.07 g, single-layered nanosheet/PVA: 0.59 ± 0.04 g, and five-layered nanosheet/PVA: 0.64 ± 0.09 g, $p > 0.1$ by ANOVA]. Blood loss 5 minutes after sealing may be summarized as follows. When only PVA films were sealed to the incised liver, blood drastically overflowed due to the PVA instantly dissolving with blood as expected, although bleeding stopped naturally 5 minutes after liver injury [Figure 4(B) closed column; blood loss: 2.60 ± 0.20 g]. On the other hand, blood loss was effectively decreased following sealing with TachoSil® (0.94 ± 0.17 g). In case of the single-layered nanosheet/PVA, arrest of bleeding was insufficient due to bursting in almost rats tested, although the nanosheet indeed adhered to the liver (2.20 ± 0.42 g). When the five-layered nanosheet/PVA was sealed, blood loss was significantly decreased because the nanosheet adhered tightly to the liver without bursting (0.65 ± 0.12 g). This hemostatic ability was almost equal to that of TachoSil®, and red blood cell count was also recovered shortly after surgical intervention, compared to PVA sealing (Figure S3). Moreover, it is noteworthy that the resected wound area sealed with the nanosheets could be seen through the transparent nanosheets, compared to TachoSil® [Figure 4(A)]. Consequently, we demonstrated that the five-layered nanosheet, which has a high bursting strength and a high level of adhesive strength, acts as a novel hemostatic dressing in a liver injury model.

Laparotomy was next carried out under lethal anesthesia 7 days after surgical intervention. Tight tissue adhesion against the liver was observed in the unspecified surrounding tissues, such as the abdominal wall, diaphragm, stomach, and/or small intestine, in all rats sealed with the PVA alone and the single-layered nanosheet, representing insufficient hemostasis [Figure 5(A)]. The severities of adhesion against liver in both groups were scored on 4.0 of a worst mark because fragile liver was easily broken, and the adhesion numbers against liver for the PVA alone and for the single-layered nanosheet were 1.6 ± 0.3 and 2.3 ± 0.3, respectively [Figure 5(B)]. When sealing with TachoSil®, severe tissue adhesion did occur to the abdominal wall and/or diaphragm existing the upper side of the liver in almost of the rats (score: 3.5 ± 0.5, number: 1.6 ± 0.4). In contrast, tissue adhesions tended to be decreased following sealing with the five-layered nanosheets (score: 2.5 ± 0.7, number: 0.8 ± 0.3). Histological observations revealed that thick fibrous membranes containing migrated fibroblasts were observed on the surfaces of the liver in the PVA and TachoSil® groups as well as the one-layered nanosheet group [Figure 5(C)]. However, almost no thickening was detected using the five-layered nanosheets [Figure 5(C)]. This suggests that the five-layered nanosheets potentially

act as a biointerface that prevents the dissemination of soluble proteins such as inflammatory and profibrotic growth factors into both the blood and surrounding tissue.

In order to consider the above phenomena, we tested the permeability of a low-molecular weight compound (Rho B) and of a protein (BSA labeled with FITC) as model analytes diffusing the five-layered nanosheets. The nanosheets were adhered onto the outside of Transwell membranes® (TMs), in which the analytes were added and set next to a 24-well plate filled with PBS [Figure 6(A)]. As a control, the TMs adhered with the single-layered nanosheet with a thickness of 59 ± 4 nm were utilized. For the bared TMs, both Rho B and BSA permeated into the outer compartments through the TMs, due to the microporous membrane [Figure 6(B)]. When the single-layered nanosheets were adhered on the TMs, permeation of Rho B was significantly decreased compared to the bared TMs [Figure 6(B)]. The permeation flux was calculated to be 22.4 g/m^2 h. These results reproduced the phenomena reported previously for the single-layered PLLA nanosheets.[29] For the five-layered nanosheets, the flux was further reduced to about one-fifth that of the single-layered nanosheets (5.0 g/m^2 h). On the other hand, BSA also permeated slightly through the single-layered nanosheets, although the flux was lower than that of Rho B [Figure 6(B), 15.5 g/m^2 h]. However, BSA barely permeated into the five-layered nanosheets, decreasing the flux to one-fortieth that of the single-layered nanosheets (0.36 g/m^2 h). Taken together, these results may indicate that the five-layered nanosheets could potentially act as a biointerface not to penetrate proteins such as growth factors in blood to support tissue repair, resulting in resistance to tissue adhesion.

DISCUSSION

We succeeded in fabricating freestanding multilayered PLLA nanosheets [Figure 1(A)]. Key points to fabricate the nanosheets are summarized as follows. First, thickness of PLLA nanosheet layers was adjusted to be about 60 nm due to the high potential to adhere to various surfaces without adhesive agents.[11] This may explain why the nanosheets with these dimensions conformed closely to surfaces, as they have an extremely flexible structure and flat surface.[11] Second, Na-Alg was selected as a sacrificial layer to fabricate multilayered nanosheets. PVA acts as an excellent water-soluble sacrificial layer to release the PLLA nanosheets from the SiO_2 substrate as reported priviously.[11–13] Moreover, we have proposed a one-pot fabrication process that uses multilayering of PVA and PLLA on the substrate to collect a large number of free-standing PLLA nanosheets.[30,31] This technique seems to be helpful to fabricate multilayered nanosheets, however, the nanosheets fabricated by using only PVA as a sacrificial layer were discretely separated when the PVA was dissolved in water.[30,31] To this end, we focused on Na-Alg, which can be converted instantly into a gel by adding divalent cations and can be redissolved by adding chelating reagents such as EDTA.[32] In fact, the multilayered nanosheets could be temporarily handled as a thick composite film when Na-Alg was converted into gels between the nanosheets. Subsequently, the thick composite film could be fusion-cut sealed by a Poly sealer® and alginate layers could be eluted by EDTA and other chelating reagents such as sodium citrate [Figure 1(A,B)]. Moreover, the thickness of alginate layers corresponds interval regions between layers of the multilayered nanosheets [Figure 1(D)]. These intervals may have significant potential to encapsulate various components for biomedical applications such as water-soluble drugs, proteins, and cells, and so forth. Third, both bottom and topmost layers of the composite film was sandwiched with hydrophilic alginate layers. Regarding the bottom layer, its hydrophilicity was necessary for easily detaching the film from the SiO_2 substrate in water. Regarding the topmost layer, we have reported that the PLLA nanosheet detached from the substrate floats on the water surface because the hydrophobic nanosheet is more stable at the air–liquid interface.[11] In fact, only the topmost layer of the film was separated and floated on the water when the topmost layer was finished with PLLA. Using this methodology, we could also fabricate multilayered nanosheets composed of versatile polymers such as polystyrene, poly(lactide-co-glycolide), polycaprolactone, and so forth. The multilayered nanosheets also offer a great advantage in time saving as a large number of nanosheets may be adhered simultaneously to various surfaces, rather than having to deposit layer upon layer of single-layered nanosheets onto the surfaces.

We demonstrated that the bursting strength of the multilayered nanosheets could be controlled by adjusting the number of layers due to increasing total thickness (Figure 2). Moreover, we found multinanolayers in the film were an important configuration to provide a high level of adhesive strength unlike thick films without multilayers (Figure 3). This mechanism can be explained as follows: The multilayered nanosheets were put on the substrate by adding a little water. The water penetrated between the layers, resulting that each layer would be separated together due to slightly residual alginate and PVA between the layers (Figure S1). During drying, the first layer of the nanosheets was directly adhered to the surface of the substrate, to which subsequent layers adhered, because individual layers could slide. In fact, the five-layered nanosheets were stably adhered to different types of surfaces such as glasses, steels, plastics, skin and organs including liver (Figure 4). They were difficult to detach even by scratching with tweezers and immersing in water for the permeation test (Figure 6). On the other hand, the single-layered nanosheets do not possess this sliding structure. As a result, the nanosheets with a thickness of over 100 nm cannot easily adhere closely together.

We demonstrated that the five-layered nanosheet acts as a novel hemostatic dressing in liver injury as well as clinically-used TachoSil® because the nanosheet adhered tightly to the liver without bursting [Figure 4(B)]. It is noteworthy that the resected wound area sealed with the nanosheets could be seen through the transparent nanosheets, compared to TachoSil® [Figure 4(A)]. It would be easy for

surgeons to judge whether or not bleeding stops after sealing with the nanosheets. Moreover, the nanosheets tended to show reduced tissue adhesion, compared to TachoSil® (Figure 5). TachoSil® is a collagen sponge containing thrombin, which promotes adequate hemostasis.[33] Conversely, it has also been reported that TachoSil® acts as a scaffold to enhance adhesion of fibroblasts, resulting in tight tissue adhesion.[19] Our results reproduced this phenomenon based on the adhesion test and the histological observation (Figure 5). On the other hand, the five-layered nanosheets may potentially act as a biointerface with resistance to tissue adhesion, in addition to their favorable hemostatic ability. We have confirmed that proteins such as thrombin and albumin were physically adsorbed on the hydrophobic surface of the PLLA nanosheets.[34] In fact, BSA barely permeated into the five-layered nanosheets (Figure 6). Blood contains abundant growth factors to support tissue repair, and it forms fibrin clots that provide a scaffold for adhesion and proliferation of fibroblasts.[35] Hence, growth factors would be adsorbed to the surface of the nanosheets adhering directly to the liver, resulting in normal wound healing. On the other hand, it is intrinsically difficult to adhere various cells to the outer surface of the bare PLLA nanosheets.[36] This can be explained by the tendency of the five-layered nanosheet's resistance to tissue adhesion. Of course, the strength of the nanosheets is also a critical aspect. In fact, the single-layered nanosheets tended to induce the unexpected adhesions more than control groups [Figure 5(B)]. This would be the reason why blood was spilled out due to bursting of the nanosheets, resulting in enhancing adsorption of proteins to induce the tissue adhesion onto the outer surface of the nanosheets. Taken together, these results support the hypothesis that the five-layered nanosheets could potentially act as a biointerface. However, the ability of the nanosheets to resist tissue adhesion was actually imperfect in this study. This is probably because small amount of blood were sometimes spilled onto the outer surface of the nanosheets from their edges while sealing. If the outer surface of the nanosheets could be modified with antifouling agents such as polymers containing phosphoryl choline groups,[37–40] the tissue adhesion properties would be much improved.

CONCLUSION

We developed a free-standing multilayered nanosheet composed of PLLA by following a simple combination procedure: (i) multilayering of PLLA and alginate, (ii) gelation of the alginate layers, (iii) fusion-cut sealing, and (iv) elution of the alginate layers. The multilayered nanosheets represent an effective configuration that not only reinforces the bursting strength but also provides a high level of adhesive strength. Furthermore, the nanosheets have the potential to act as a new hemostatic dressing, as they tended to show decreased tissue adhesion in liver injury. Hence, we propose this biomaterial as an ideal candidate for an alternative to conventional therapy for the liver and other operations accompanied by bleeding.

ACKNOWLEDGMENTS

The authors wish to thank Dr. Akira Katoh at the Institute of Innovative Science and Technology, Tokai University, for valuable discussions of statistical analyses, Technical Service Coordination Office, Tokai University, for technical support of SEM observations, and Support Center for Medical Research and Education, Tokai University, for technical support regarding *in vivo* experiments.

REFERENCES

1. Cheng W, Campolongo MJ, Tan SJ, Luo D. Freestanding ultrathin nano-membranes via self-assembly. Nano Today 2009;4:482–493.
2. Nikoobakht B, Li X. Two-dimensional nanomembranes: Can they outperform lower dimensional nanocrystals? ACS Nano 2012;6: 1883–1887.
3. Mallwitz F, Laschewsky A. Direct access to stable, freestanding polymer membranes by layer-by-layer assembly of polyelectrolytes. Adv Mater 2005;17:1296–1299.
4. Tang ZY, Kotov NA, Magonov S, Ozturk B. Nanostructured artificial nacre. Nat Mater 2003;2:413–418.
5. Eck W, Küller A, Grunze M, Völkel B, Gölzhäuser A. Freestanding nanosheets from crosslinked biphenyl self-assembled monolayers. Adv Mater 2005;17:2583–2587.
6. Endo H, Mitsuishi M, Miyashita T. Free-standing ultrathin films with universal thickness from nanometer to micrometer by polymer nanosheet assembly. J Mater Chem 2008;18:1302–1308.
7. Vendamme R, Onoue SY, Nakao A, Kunitake T. Robust free-standing nanomembranes of organic/inorganic interpenetrating networks. Nat Mater 2006;5:494–501.
8. Fujie T, Okamura Y, Takeoka S. Ubiquitous transference of a free-standing polysaccharide nanosheet with the development of a nano-adhesive plaster. Adv Mater 2007;19:3549–3553.
9. Fujie T, Okamura Y, Takeoka S. Selective surface modification of free-standing polysaccharide nanosheet with micro/nano-particles identified by structural color changes. Colloids Surf A 2009;334:28–33.
10. Fujie T, Matsutani N, Kinoshita M, Okamura Y, Saito A, Takeoka S. Adhesive, flexible, and robust polysaccharide nanosheets integrated for tissue-defect repair. Adv Funct Mater 2009;19:2560–2568.
11. Okamura Y, Kabata K, Kinoshita M, Saitoh D, Takeoka S. Free-standing biodegradable poly(lactic acid) nanosheet for sealing operations in surgery. Adv Mater 2009;21:4388–4392.
12. Okamura Y. Fabrication of ultra-thin nanosheets with unique properties for biomedical applications. Kobunshi Ronbunshu 2013;70:351–359.
13. Okamura Y, Nagase Y. Fabrication of bio-friendly polymer nanosheets for biomedical applications. Trans Mat Res Soc Japan 2014;39:379–384.
14. Conn J Jr, Oyasu R, Welsh M, Beal JM. Vicryl (polyglactin 910) synthetic absorbable sutures. Am J Surg 1974;128:19–23.
15. McGuire DA, Barber FA, Elrod BF, Paulos LE. Bioabsorbable interference screws for graft fixation in anterior cruciate ligament reconstruction. Arthroscopy 1999;15:463–473.
16. Kumari A, Yadav SK, Yadav SC. Biodegradable polymeric nanoparticles based drug delivery systems. Colloids Surf B: Biointerfaces 2010;75:1–18.
17. Vasir JK, Labhasetwar V. Biodegradable nanoparticles for cytosolic delivery of therapeutics. Adv Drug Deliv Rev 2007;59:718–728.
18. Ueda N, Maekawa Y, Ohtani H, Uchiyama H, Kashiwabara S, Koshiyama Y, Oda M, Kurumi M. Hemostatic effect of a novel sheeted fibrin adhesive agent, TO-193, on experimental incision model. Nihon Yakurigaku Zasshi 1999;113:177–184.
19. Niwa D, Koide M, Fujie T, Goda N, Takeoka S. Application of nanosheets as an anti-adhesion barrier in partial hepatectomy. J Biomed Mater Res B 2013;101:1251–1258.
20. Markutsya S, Jiang C, Pikus Y, Tsukruk VV. Freely suspended layer-by-layer nanomembranes: Testing micromechanical properties. Adv Funct Mater 2005;15:771–780.
21. Baba S, Midorikawa T, Nakano T. Unambiguous detection of the adhesive failure of metal films in the microscratch test by

waveform analysis of the friction signal. Appl Surf Sci 1999;144–145:344–349.
22. Ohya S, Sonoda H, Nakayama Y, Matsuda T. The potential of poly(*N*-isopropylacrylamide) (PNIPAM)-grafted hyaluronan and PNIPAM-grafted gelatin in the control of post-surgical tissue adhesions. Biomaterials 2005;26:655–659.
23. Okamura Y, Goto T, Niwa D, Fukui Y, Otsuka M, Motohashi N, Osaka T, Takeoka S. Fabrication of free-standing albumin-nanosheets having heterosurfaces. J Biomed Mater Res A 2009;89:233–241.
24. Okamura Y, Utsunomiya S, Suzuki H, Niwa D, Osaka T, Takeoka S. Fabrication of freestanding nanoparticle-fused sheets and their hetero-modification using sacrificial film. Colloids Surf A 2008; 318:184–190.
25. Auriemma G, Del Gaudio P, Barba AA, d'Amore M, Aquino RP. A combined technique based on prilling and microwave assisted treatments for the production of ketoprofen controlled release dosage forms. Int J Pharm 2011;414:196–205.
26. Frank DW. Physiological data pf laboratory animals. In: Melby ECJ, editor. Handbook of Laboratory Animals Science. Boca Raton, FL: CRC Press; 1976. p 23–64.
27. Sou K, Klipper R, Goins B, Tsuchida E, Phillips WT. Circulation kinetics and organ distribution of Hb-vesicles developed as a red blood cell substitute. J Pharmacol Exp Ther 2005;312:702–709.
28. Masyuk TV, Ritman EL, LaRusso NF. Hepatic artery and portal vein remodeling in rat liver. Am J Pathol 2003;162:1175–1182.
29. Fujie T, Kawamoto Y, Haniuda H, Saito A, Kabata K, Honda Y, Ohmori E, Asahi T, Takeoka S. Selective molecular permeability induced by glass transition dynamics of semicrystalline polymer ultrathin films. Macromolecules 2013;46:395–402.
30. Okamura Y, Kabata K, Kinoshita M, Miyazaki H, Saito A, Fujie T, Ohtsubo S, Saitoh D, Takeoka S. Fragmentation of poly(lactic acid) nanosheets and patchwork treatment for burn wounds. Adv Mater 2013;25:545–551.
31. Okamura Y, Nagase Y, Takeoka S. Patchwork coating of fragmented ultra-thin films and their biomedical applications in burn therapy and antithrombotic coating. Materials 2015;8:7604–7614.
32. Alvarez-Lorenzo C, Blanco-Fernandez B, Puga AM, Concheiro A. Crosslinked ionic polysaccharides for stimuli-sensitive drug delivery. Adv Drug Deliv Rev 2013;65:1148–1171.
33. Rickenbacher A, Breitenstein S, Lesurtel M, Frilling A. Efficacy of TachoSil a fibrin-based haemostat in different fields of surgery—A systematic review. Expert Opin Biol Ther 2009;9:897–907.
34. Okamura Y, Schmidt R, Raschke I, Hintze M, Takeoka S, Egner A, Lang T. A few immobilized thrombins are sufficient for platelet spreading. Biophys J 2011;100:1855–1863.
35. Barrientos S, Stojadinovic O, Golinko MS, Brem H, Tomic-Canic M. Growth factors and cytokines in wound healing. Wound Repair Regen 2008;16:585–601.
36. Niwa D, Fujie T, Lang T, Goda N, Takeoka S. Heterofunctional nanosheet controlling cell adhesion properties by collagen coating. J Biomater Appl 2012;27:131–141.
37. Ishihara K, Ueda T, Nakabayashi N. Preparation of phospholipid polymers and thier properties as polymer hydrogel membranes. Polym J 1990;22:355–360.
38. Iwasaki Y, Yamasaki A, Ishihara K. Platelet compatible blood filtration fabrics using a phosphorylcholine polymer having high surface mobility. Biomaterials 2003;24:3599–3604.
39. Sakagami Y, Horiguchi K, Narita Y, Sirithep W, Morita K, Nagase Y. Syntheses of a novel diol monomer and polyurethane elastomers containing phospholipid moieties. Polym J 2013;45:1159–1166.
40. Sirithep W, Morita K, Iwano A, Komachi T, Okamura Y, Nagase Y. Syntheses and properties of elastic copoly(ester-urethane)s containing a phospholipid moiety and the fabrication of nanosheets. J Biomater Sci Polym Ed 2014;25:1540–1557.